Stereology for Multitemporal Images with an Application to Flooding

Alfred Stein, Petra Budde, Mamushet Zewuge Yifru

ITC, PO Box 6, 7500 AA Enschede, The Netherlands

Abstract

This paper presents stereology for flooded areas observed on a multitemporal remote sensing image. Stereology is a mathematical method to quantify objects at one dimension from simulated objects at a lower dimension. It was initially developed for geological and soil objects. Here it is applied to objects on multitemporal remote sensing images, i.e. for image mining. Image mining considers the chain from object identification from remote sensing images through modeling, tracking a series of images and prediction, towards communication to stakeholders. The paper introduces the estimation of the area size of the same object observed at various moments in time. It is illustrated with a case study on flooding of the Tongle Sap lake in from Cambodia.

1 Introduction

Remote sensing images are available at an increasing frequency and spatial resolution and from a large variety of sensors. Monitoring is thus increasingly benefitting from the presence of satellites. Commonly a spatial object is identified, and several of its properties are followed in time. Examples are the monitoring of cities, monitoring forests and of deforestation,

G. Navratil (eds.), *Research Trends in Geographic Information Science*,
Lecture Notes in Geoinformation and Cartography, DOI 10.1007/978-3-540-88244-2_10,

and the monitoring of drought. Apparently, both spatial and temporal dimensions have their own uncertainties: observation of the area is usually not done continuously, whereas the object can be uncertain at each moment of observation. Simply following an object is usually not sufficient for decision making. A division can thus be made into the signaling of threshold exceedance and the spotting of unexpected events, such as landslides and outbreak of pests in an agricultural field. The information thus collected has as a requirement that it is communicated to stakeholders. Image mining has been shown to be a useful system for doing so. Despite this development, uncertainty is still largely present, and information should be communicated as condensed as possible. In this regard, uncertainty plays a critical role as well, being both a problem and an asset to spatial information (Frank 2008).

We thus increasingly see it as an important step to summarize the information of spatial objects in a quantitative way. For any spatial object both geometrical properties and attributes are to be considered. In the recent past, measuring the size of an object was an important and relevant step. Spatial data quality is a cornerstone in this area, quantifying lack of quality caused by mis-classification, poor object definition and timeliness of the data. This has resulted in the development of spatial data quality as a scientific discipline (Shi 2009; Stein et al. 2008). We realize, however, that with the increasing amount of information *in time* the need is increasing to better quantitatively assess this information. In a risk analysis, for example, a long lasting disaster may have a much larger impact, say on crop production, than a short one, although both can be equally devastating.

In this study, we use stereology for multitemporal remote sensing images, focusing on estimation of 2D objects. The more general approach to estimate 2D × T objects will be postponed to another paper. Stereology is an unbiased and effective tool to obtain quantitative 2D geometric properties (e.g., number, length, area, volume etc.) from recorded series of sections in a lower dimension. Stereology can be stated as a method for solving the problem of measuring a physical object in n dimensions from random measured objects in less dimensions (Baddeley 1991; Baddeley and Vedel Jensen 2005). In an earlier paper (Stein et al., 2009) we focus on 2-dimensional objects on a single image. We now extend this approach towards multitemporal images. To do so, we turn towards image mining.

Image mining is a relatively new development focusing on extracting relevant information from large sets of remote sensing images (Stein 2008; Silva et al. 2008). It can be defined as "The analysis of (often large sets of) observational images to find (un)suspected relationships and to summarize the data in novel ways that are both understandable and useful to stakeholders". Image mining in space has as a focus to combine a large set of similar images, in order to identify similar objects. In space, it concerns the

classification and segmentation, for example using textural image segmentation as a first step, to identify for example forest fires, flooded parcels, deforested patches or sub-areas of a rich biodiversity. Its main objective is to reduce uncertainty, allowing making better decisions (Frank 2008). An important step during image mining is thus the identification of spatial patterns and testing of their significance. Image mining recognizes issues of data quality as a crucial element. Data quality depends upon the fitness for use, i.e. the required decision and hence on the stakeholders' interests.

The aim of this paper is to present essentials of stereology towards analysis on multitemporal remote sensing images. The study is illustrated with an example from flooding in Cambodia.

2 Stereology

2.1 Basics

Stereology is an unbiased and effective tool to obtain quantitative geometric properties like number, length, area and volume from recorded series of sections of a lower dimension (Vedel Jensen 1998). It can be used to measure a physical object in n dimensions from randomly measured objects in fewer dimensions. It is based on Delesse (1848) who applied it to determine the volume of a number of minerals in rocks. He showed that the areal fraction occupied by a given mineral on the section of a rock AA is proportional to the volume fraction of the mineral within the rock volume VV. This notation identifies A or V as the object dimension of interest, and the subscripts as the dimension of the sampling unit (Baddeley 1991; Baddeley and Vedel Jensen 2005). A basic principle of stereology is Cavalieri's principle (Cavalieri 1635): "if two solid objects have equal plane sections on all the intersecting planes (A_h, $h \in T$), then the objects have equal volume". The principle of stereological measurement is by taking the geometry and probability statistics of an object into consideration. One can consider estimation of the area of an object within a window by allocating, say, m random test points to that window and using the fraction of points that falls on the object as a measure of the proportion of the object covering the window, and hence as a measure for the area of the object. Similarly, one can randomly distribute m random test lines to the window and the fraction of those lines within the object gives an estimate of the proportion of the object falling within the window. These two examples are typically two-dimensional, but stereology is applicable to any set of dimensions. For a 1-dimensional line object, containing a line fragment of interest, one may allocate random points and count the fraction of points falling on the segment and have that as the fraction of the line

fragment to the line object. In a 3 dimensional window, interest may be on a 3D object, covering a part of that window and one may wish to estimate the fraction of the window occupied by that object. This volume could be either estimated by allocating random points, or random lines, or random planes inside the window. Similarly, when interest concerns a surface, the area of the surface could be estimated by allocating random lines in the window and identifying the number of intersecting points.

Two important concepts in stereology are its unbiasedness and the way of taking samples. Unbiasedness implies that by taking enough samples the calculated property of the volume gives the population value. Stereological estimators are unbiased estimators. Sampling concerns the choice of the sampling objects within the window. This gives a distinction between classical and modern stereology. On the one hand, classical stereology, or model-based stereology, is based on the assumption that the material is homogeneous in composition, i.e. a geometric assumption about the structure of the object (Baddeley 1991; Ross and Dehoff 1999). On the other hand, design-based stereology requires no assumptions regarding the geometric aspect of the feature of interest, such as its shape, its size, and its orientation, as well as by the use of systematic random sampling procedures. Design-based stereological sampling relies mainly on systematic sampling (Glaser and Glaser 2000). For example, a test line is selected randomly and the sample is assumed to be arbitrary and fixed. These ensure that each feature of interest in the specimen has an equal probability of being sampled (Baddeley and Vedel Jensen 2005). Design-based stereology is effective and suited in estimating global and nonhomogeneous populations (Baddeley and Vedel Jensen 2005). Like model-based stereology it results in an unbiased estimate of a high precision of geometric quantities like volume, surface area or perimeter of an object.

Applications of stereological techniques are useful in a broad variety of disciplines, such as, in biological, medical, material science, food science, and other fields. So far, much research has been done in the field of biomedical science to estimate quantitative information about 3D microscopic structures, based on 2D observations, especially to obtain a deeper understanding of the structure and function of human body cells and a more objective diagnosis of progressive disease assessment (Roberts et al. 2000). Stereology has also been used as a precise, simple and efficient means of quantifying three-dimensional microscopic structures from two-dimensional quantitative sections. Stereological volume estimations are also applied as sums of measurements of serial sections performed on sampling areas measured on thin sections (Dorph-Petersen et al. 2000; Kötzer 2006). But so far, applications of stereology to remote sensing images have been missing and it is little known in geoinformation science (see Stein et al. 2009 for a short introduction).

2.2 Identifying 2D Objects from Images

In this study we aim to use stereology within an image mining as stereology may serve as an opportunity to handle the large amount of data thus collected. In our study we consider 2D objects of which we estimate the area using random straight lines, i.e. an L_L estimation.

Stereology extracts structural quantities from measurements made on 2D images: the surface area (S) of a 2D object, the length of lines (L) and number of points (n). We apply the standard notation of the objects together with their subscripts indicate the way that the measurements are made with respect to this object. Subscripts indicate the type of measurements that have been used, for example, measurements on an image per volume area have a subscript $._A$. Stereology thus considers S_V as a specific surface area of a volume, for example the surface of a 3D object per unit volume of this object. Similarly, L_V is a specific line length of (length per unit volume) of a curve or line structure. This applies as well to the length per area L_A as the length per unit area for a 2D object, the number of points per area unit n_A, n_L as the number of points per linear unit and A_A as the (dimensionless) area fraction per unit area.

Table 1. Notation for geometrical properties (after Baddeley 1991)

Dimension	set X	Symbol	Meaning
Space (2D)	Plane domain	A	Area
	Curve	L	Curve length
	Finite set of points	P	Number of points
	Finite set of objects	Q	Number of objects
	Curve	C	Total curvature

We next move towards estimation and we do this by the use of test lines. In doing so, we may consider linear objects, for example the length of a perimeter of an object on an image can be determined from the number of times it meets a straight line and the length of a curve that can be determined from the number of intersection points it makes with random lines. Common stereology estimators are denoted as $\hat{L}$ as an estimator for the length of a line per unit area, $\hat{A}_A$ as the surface area estimator per unit area, $\hat{L}_L$ as the area estimator for the length per unit length, etc. and $\hat{V}$ as the volume estimator. Table 2 shows basic stereological formulae for expected measurable parameters.

Table 2. Basic stereological formula for expected measurable parameters.

	Dimension			
	3	2	1	0
0	$\hat{V}_V$	$\hat{A}_A$	$\hat{L}_L$	$\hat{P}_P$
1	$\hat{S}_V$	$\frac{4}{\pi}\hat{L}_A$	$2\hat{P}_L$	
2	$\hat{L}_V$	$2\hat{Q}_A$		

2.3 Remote Sensing Images

We now consider an individual remote sensing image and we identify a region of interest with the object and the image in full with the window. A sharp and unambiguous identification of the object is determined by different factors, such as atmospheric conditions, time of observation. Moreover, the spatial resolution of an image is limited, leading to a blocky structure when zooming in, and also the definition of the object may be such that it is only vaguely defined. Moreover, the object may show internal variation and its identification and classification is subject to various uncertainties. At this stage, however, we will not venture too much into issues of data quality, but will focus on an object that is clearly identifiable, relatively homogeneous, of a sufficiently high resolution, and where atmospheric distortion is virtually absent. Interest will focus on determining the size of the area, and estimation will be done by random lines. When using a stereological estimator, the number of lines has to be decided upon in advance. This depends largely upon the desired quality. An increasing number of lines will lead to an increasingly precise estimate. As no general statements are given, we will make it part of this research.

2.3.1 Image Mining

Image mining (Stein 2008; Pereira dos Santos Silva et al. 2008), considers the analysis of observational images to find (un)suspected relationships and to summarize the data in novel ways that are both understandable and useful to stakeholders (Fig. 1). Objects representing earth processes discernable on those images can be either crisp or fuzzy and vague.

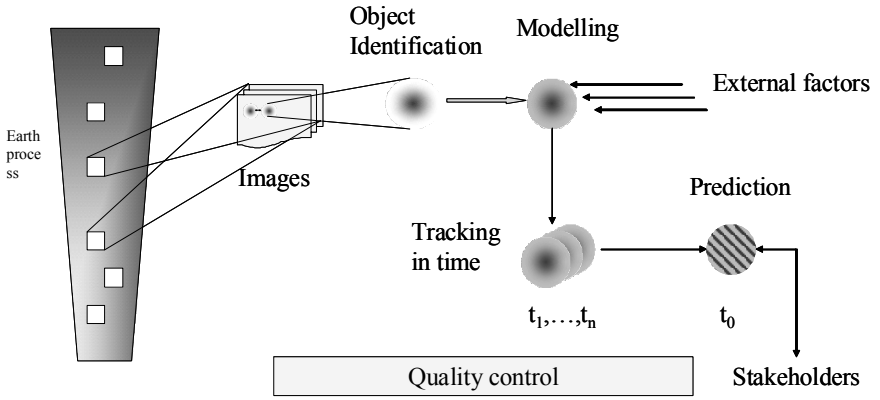

Fig. 1. Image mining of spatial and temporal earth processes.

We distinguish five key steps in image mining: identification, modeling, tracking, prediction and communication with stakeholders. All these steps will be briefly discussed below. On top of this, we notice aspects of spatial data quality in each of these steps.

Identification of an object requires making the step from raster to objects by grouping grid cells with similar digital numbers into one object. That is usually done by applying an image segmentation technique. Procedures for image segmentation are well documented, e.g. based on mathematical morphology, edge detection, identifying homogeneity in one band or in a set of bands, and on texture based segmentation (Glasbey and Horgan 1995; Ojala and Pietikäinen 1999; Lucieer et al. 2005). This may include as well uncertainty values. Segmentation is followed by a classification towards a set of object classes (Richards et al. 1998). Considering 2 classes at the moment (the pixel belongs to the object, or the pixel does not belong the object), this results in an object X and the remainder of the window X^c. Image mining next considers modeling of this object. As our primary focus is on geometrical aspects, however, we will not proceed further here (see Stein 2008). Also the tracking of objects, i.e. following of the object in time, will not be explored in all detail. For multitemporal images, it is sufficient at this stage to restrict ourselves to objects that are well identified and correspond physically to objects at earlier stages. In fact, the objects are observed as snapshots of a process. It may be important in image mining to predict properties of an object at a moment t_0 beyond the observation period. This can be done by a parametric curve for the centroid and other parameters, e.g., by a linear statistical model (Rajasekar et al. 2006). The final stage concerns communication to stakeholders. Various ways exist here, ranging from simple visualization towards assessments of costs and benefits. Issues from decision support typically are required here (Van

de Vlag and Stein 2006). In our study exploring the possibilities of stereology, we will aim to communicate directly the area of an object as a number, possibly summarized by some simple graphical output.

2.3.2 Application

This application considers flooding of the Tonle Sap Great Lake in Cambodia (Fujii et al. 2003). The study area lies on the lower part of Mekong region of Cambodian floodplain following the Mekong river (Fig. 2). The country is characterized by five distinct topographic features: the sandstone Dangrek range in the north, forming the border with Thailand, the granite Cardamom Mountains with peaks of over 1500 m in the southwest, the Darlac Plateau which rises to over 2700 m and in the north-east and the Central Plains between 10 and 30 m above sea level, which form 75% of the Cambodian land area. Flooding due to high water levels of the Mekong River and its tributaries recurs yearly. It causes a considerable damage on human settlements, agricultural activities and infrastructures of the surrounding area. The Tonle Sap Great Lake covers a relatively small area in the dry season and increases to three to four times this area during the wet season. The study area is bounded within a box with the coordinates 12°06'25" N to 13°55'56" N and 102°29'13" E to 104°28'51" E.

Application of remote sensing to a flooded area in a densely vegetated area identifies the object of study by reflectance values that deviate from those in its neighborhood. Starting from May 2001 to January 2002, a series of 9 Landsat 7 ETM+, multi-spectral images were used. The area extent of the lake varies depending on the observation time. Images were collected on the following dates: 31 May (Early flood), 16 June (Early flood), 2 July (Early flood), 18 July (Start of rising flood), 3 August (Rising flood), 4 September (Rising to peak flood), 20 September (Peak flood), 23 November (Peak to falling flood) and 10 January (Falling flood stage). These moments were determined by visibility of the lake from the Landsat 7 ETM+ sensor: only images that contained less than 15% clouds were useful.

The stereological test system for this study consists of test lines, a known frame (i.e., the full images) and 9 incidentally recorded satellite images for information extraction. In this particular stereological test system, we equate the flood to our feature of interest Y_t, $t = 1,\ldots,9$ in the spatial domain R^2, and we equate the survey area with X_t, $t = 1,\ldots,9$. Apparently, $X_t \subset R^2$ contains a subset $Y_t \subset X_t$.

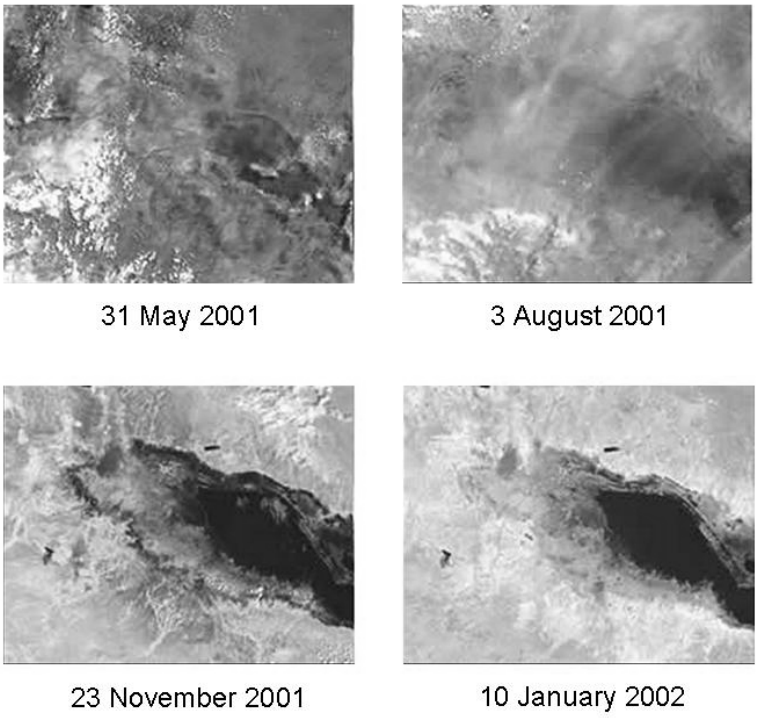

Fig. 2. Four Landsat images of the process of flooding around the Tonle Sap Great Lake in Cambodia during the 2002 rainy season (Yifru 2006).

We describe image mining for 'flooded area' as follows. At t_1 = May 31st we observe n_1 objects: one large object and a series of n_{1-1} small objects, characterized as $X_{1,i}$, i = 1,..., n_1 and we have $X_1 = \bigcup_{i=1}^{n_1} X_{1,i}$ (Fig. 3). There is little change as compared to t_2 = June 16th. The objects $X_{1,i}$ can simply be tracked to objects $X_{2,i}$, equating objects at similar position but at different moments in time with each other. As before, $X_2 = \bigcup_{i=1}^{n_2} X_{2,i}$. At t_3 = July 2nd, some of the smaller objects expand, and some objects merge yielding one large and several small objects. Understanding the flooding process requires a careful tracking to relate the n_3 objects at t_3 with the n_2 objects at t_2. We also notice the birth of several new objects. At t_4 = July 18th, the large object is increasing further and one of the objects at t_3 is decreasing and splitting into some smaller objects. Changes from t_4 to t_5 are small, but we

observe a decrease in the size of the largest object. At t_6 = September 4th we notice that the objects have now merged into a single large object, labeled as $X_{6,1}$, which we also observe as the single object $X_{7,1}$ at t_7 = September 20th, being of a somewhat smaller size. During the next period the flooding apparently reduces and at t_8 = November 23rd we notice a reduction in the size of $X_{7,1}$ to become $X_{8,1}$ and the birth of several, say n_8 - 1 smaller objects. At t_9 = January 10th, we notice that the largest object, now labeled $X_{9,1}$ is of a comparable size as at t_1 but of a somewhat different shape. At all each moment t the object of interest equals $X_t = \bigcup_{i=1}^{n_t} X_{t,i}$.

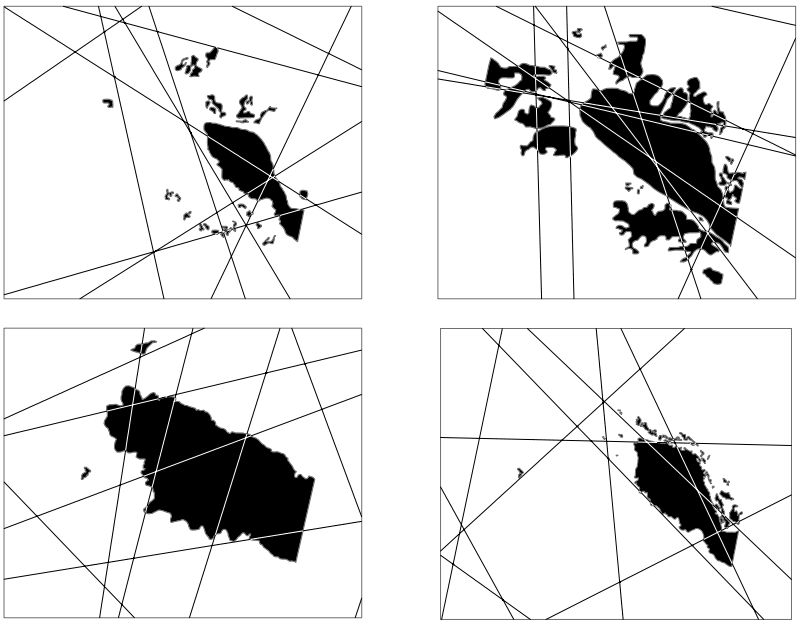

Fig. 3. Four flooding objects extracted from the Landsat images around the Tonle Sap Great Lake in Cambodia during the 2002 rainy season. Random lines are drawn to estimate the area size.

We use stereology to identify the size of the different lakes on each of the images. Initially we used m = 1000 lines for the estimation. As an example, we show 10 of such liens drawn at random at each of the four instances (Fig.4).

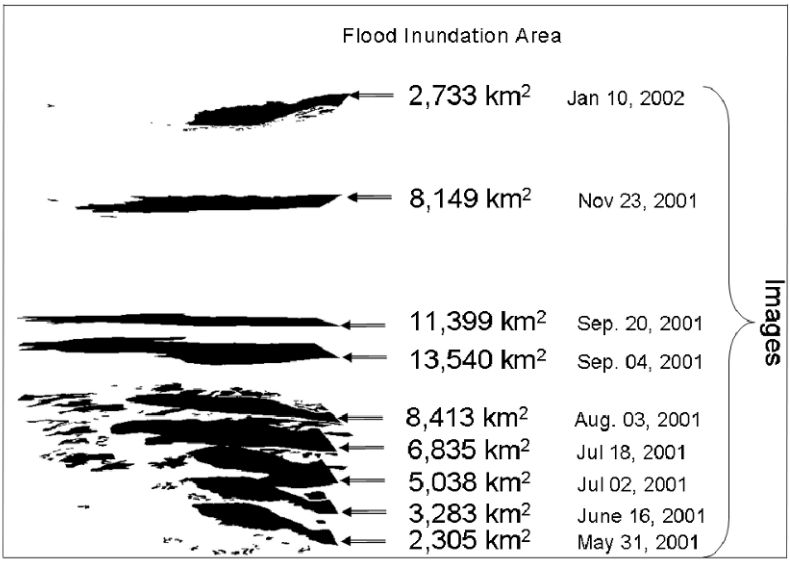

Fig. 4. Flooding objects identified in the Tonle Sap Great Lake area at the 9 moments of observations.

	31-5	6-6	2-7	18-7	3-8	4-9	20-9	23-11	10-1
Area									
Mean	0.0534	0.0767	0.1171	0.1558	0.1943	0.3128	0.2638	0.1887	0.0634
Mean (km^2)	2337	3334	5078	6757	8440	13497	11409	8154	2752
Min	0.0516	0.0737	0.1131	0.1500	0.1884	0.3062	0.2529	0.1820	0.0601
Max	0.0556	0.0805	0.1217	0.1621	0.2014	0.3220	0.2737	0.1997	0.0663
Max (km^2)	2396	3472	5248	6989	8687	13889	10908	8611	2590
Sd.	0.0009	0.0013	0.0017	0.0024	0.0024	0.0031	0.0033	0.0027	0.0013
Observed	0.0542	0.0773	0.1177	0.1567	0.1957	0.3130	0.2645	0.1891	0.0638
Error									
Mean (km^2)	36	29	28	39	60	9	30	16	20
Max (km^2)	59	138	170	232	247	392	501	457	162

Estimates of the area size obtained with 1000 random lines as proportion of the window and in km^2; the error is expressed as the difference between expected and worst estimate of 100 simulations.

We notice that the estimates are precise, with standard deviations equal to approximately 2 % and measured and average of the simulations very close (within the mean ± 2 × sd). This applies to all of the different dates for which observations were available. As the size of the lake is big, however, we notice that the differences as expressed in km^2 are substantial: on the average (for the 100 simulations) it ranges to areas of 9 to 40 km^2, whereas maximum values equal to more than 500 km^2 may emerge.

Fig. 5 shows for each time the empirical densities of the distribution of the surface areas and the $N(\mu_t,\sigma_t)$ densities at $t = 1,\ldots,9$ obtained with 100 estimates. We notice that differences can be substantial, for example at September 20th the empirical distribution shows more variation than could be represented by a normal distribution. It leads to the conclusion that a set of 100 lines (or less) may not be adequate to derive properties of the area.

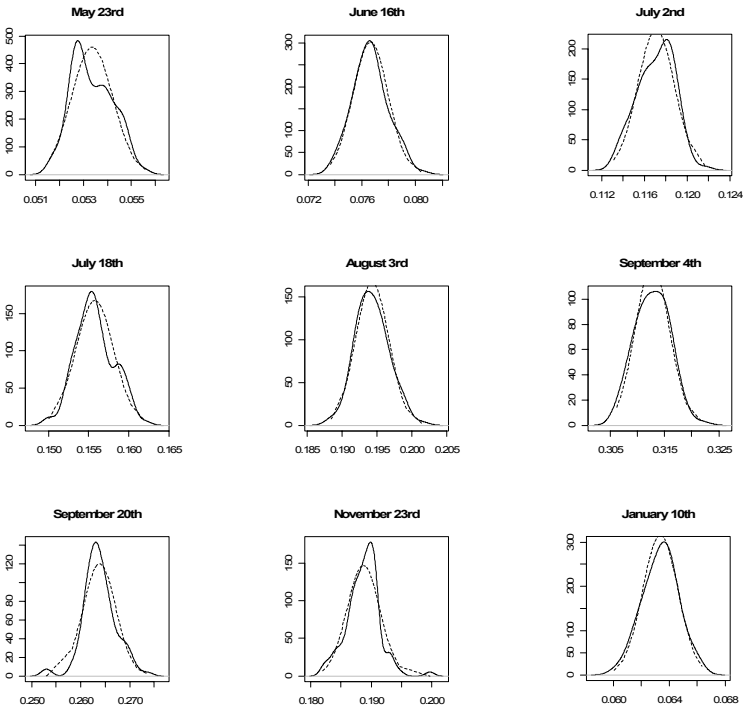

Fig. 5. Estimated densities and corresponding Normal distributions obtained with 100 estimated lines.

One question that we tried to answer with this study was the number of simulations necessary to do these calculations. Hence we did the calculations also with less random lines, leading to the results shown in Fig. 6.

We notice an expected gain in precision, for example expressed by the length of the whiskers. The number of $m = 1000$ lines may be sufficient for various purposes, but to obtain even better estimates this number may be further increased. We have to realize, though, that the limited resolution of the images may put a limit to the increase in precision. A number of m below 1000 seems not to be very attractive, and may result into unnecessary uncertainty, in particular as computation time for these objects is short.

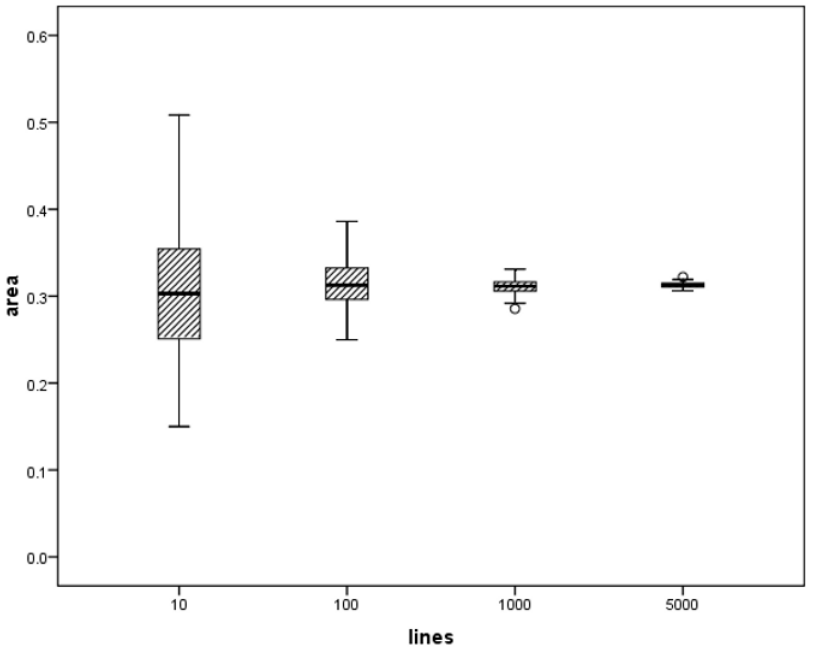

Fig. 6. Effect of the number of lines on the precision of the areal estimate.

3 Discussion

Stereology as it was developed during the last decades seems to be of interest to be applied to multitemporal images. It offers many possibilities to estimate geometrical aspects of spatial objects. With the further sophistication of image processing software, the possibilities might be further explored. In this study, we applied random lines for area estimates, but similar estimates might have been applied to a range of different other parameters, like the perimeter of an object, the length of the largest diameter, or simply the number of sub-objects constituting the single object as analyzed so far.

Stereological estimates may also play a role in data quality issues. Spatial data quality affects GIS based decision making activity (Shi et al. 2002). When using data as an input in numerical models, data precision should be taken care of, in particular if it propagates towards the decision. In this study, the accuracy of stereologically estimated 2D area by passing different set of lines (10, 100, 100, and 5000) depends upon the number of

lines drawn to quantify the area and the lines passing through the image should be selected at random. It remains to the user of information, however, which precision is required. A land planner may be satisfied with a relatively coarse number, whereas an individual inhabitant of the area might require a much higher precision to have information about his ground at a sufficiently precise level.

Spatial data quality refers to various aspects of data quality as can be identified for in geographical objects. Although various aspects can be considered, we restrict ourselves to the two main components in this paper, namely positional accuracy and attribute accuracy. Apparently the two are closely related to each other. For uncertain objects, positional accuracy is dealt with by characteristics of the membership function, such as the support of a fuzzy set, the shape of the membership function and characteristics of its α-shapes. The attribute accuracy is identified by the content of the membership function, i.e. its relation towards the object under study. It basically answers the question to which degree the membership function expresses the concepts that are displayed. Extension of stereology to these objects has to be done.

The algorithm has been implemented in a Python environment. Estimators in the implemented algorithms from the competition of fraction of each line lying within the object representing the flooded area. To estimate a 2D area it counts the pixels on those lines for the case of 2D area estimation. The general trend of the stereologically estimated 2D area enable us at what time interval a significant change in the pattern occurs.

Flooding apparently is one of the phenomena that we can characterize using stereology in an image mining context. It starts at some moment in time, it may be poorly visible at several moments in time, because of (partial) cloud cover, it increases in size, it may split, several objects may merge, and after the river withdraws, the flood ends and the object reduces to its original size. Moreover, also the boundaries between flooded and non-flooded land are difficult to draw, if possible at all and (partial) cloud cover may prohibit its precise and detailed observation. Flooding can further be interpreted from information from various perspectives like natural, ecological, environmental or socio-economical information. It is a further challenge to include this all into the stereological context.

4 Concluding Remarks

We conclude from this study that stereology presents a set of estimators that are very helpful to estimate geometrical properties of objects that are clearly and unambiguously identifiable from remote sensing images. Thus

stereology could provide a valuable set of tools to be generally applicable in image mining. It has been shown to be applicable for area estimation by random line objects, whereas an extension to other properties by different estimators is applicable as well. In particular, estimation of area sizes by allocating random points might be simply applicable. Of slightly more interest may be the estimation of the length of linear objects, such as roads and rivers, by applying random lines. This would require a careful analysis of multiple hits, but we believe that it is solvable. Estimated values can be of any precision, restricted by the limited resolution of the images and by computation time, which has been short for this study.

For the application considered in this study, there is a clear indication that the number of applied random lines is satisfactory when considering the fraction of the area that is flooded, but that the size of that area expressed in km^2 may be of a too low precision for many practical purposes. In the future we aim to further explore possibilities for extending stereological estimators into the space-time domain.

At this stage, we could imagine that research questions to be resolved are primarily of a topological nature, i.e. the lengths and areas of objects. But after some extension, it might be possible as well to consider uncertain objects and research could extend towards identifying fuzziness of such objects, for example by selecting α shapes for several values of α, and translating areas (or lengths) thus identified towards object sizes for the same values of α. Further research is needed in these directions. A possibly interesting research direction could also be towards separability of classes when the number of classes is larger than 2. It is not difficult to imagine that class overlap may lead to ambiguity in topological properties, and robust solutions should be provided.

References

Baddeley A (1991) Stereology. In: Spatial Statistics and Digital Image Analysis, chapter10, National Research Council USA, Washington DC

Baddeley A, Vedel Jensen EB (2005) Stereology for statisticians, Chapman and Hall/CRC 395, Boca Raton London

Cavalieri B (1635) Geometria indivisibilibus continuorum. Bononi: Typis Clementis Ferronij, Reprinted 1966 as Geometria Degli Indivisibili, Unione Tipografico-Editrice Torinese, Torino

Delesse MA (1848) Procéedé mechanique pour determiner la composition des roches. Annales des Mines 13, Quatrième série: 379–388

Dorph-Petersen KA, Gundersen HJG, Jensen EBV (2000) Non-uniform systematic sampling in stereology. Journal of Microscopy 200: 148–157

Frank AU (2008) Analysis of Dependence of Decision Quality on Data Quality. Journal of Geographical Systems 10(1): 71–88

Fujii H, Garsdal H, Ward P, Ishii M, Morishita K, Boivin T (2003) Hydrological roles of the Cambodian floodplain of the Mekong River. International Journal of River Basin Management 1(3): 1–14

Glaser J, Glaser EM (2000) Stereology, morphometry, and mapping: the whole is greater than the sum of its parts. Journal of Chemical Neuroanatomy 20: 115–126

Glasbey C, Horgan R (1995) Image analysis for the biological sciences, Wiley, Chichester

Kötzer S (2006) Geometric identities in stereological particle analysis. Image Analysis and Stereology 25(2): 63–74

Lucieer A, Stein A, Fisher P (2005) Multivariate Texture Segmentation of High-Resolution Remotely Sensed Imagery for Identification of Fuzzy Objects. International Journal of Remote Sensing 26: 2917–2936

Ojala T, Pietikäinen M (1999) Unsupervised texture segmentation using feature distributions. Pattern Recognition 32: 477–486

Pereira dos Santos Silva M, Camara G, Sobral Eescada MI, Modesto de Souza RC (2008) Remote-sensing image mining: detecting agents of land-use change in tropical forest areas. International Journal of Remote Sensing 29(16): 4803–4822

Rajasekar U, Stein A, Bijker W (2006) Image mining for modeling of forest fires from Meteosat images. IEEE Transactions on Geoscience and Remote Sensing 45(1): 246–253

Richards JA, Jia X (1998) Remote sensing digital image analysis - third edition, Springer, Berlin Heidelberg New York

Roberts N, Puddephat MJ, McNulty V (2000) The benefit of stereology for quantitative radiology. British Journal of Radiology 73: 679–697

Shi W (2009) Principles of modelling uncertainties in spatial data and spatial analysis, CRC Press, Boca Raton

Shi W, Fisher PA, Goodchild M (2002) Spatial Data Quality, Taylor & Francis, London

Stein A (2008) Modern developments in image mining. Science in China Series E: Technological Sciences 51: 13–25

Stein A, Shi W, Bijker W (2008) Quality aspects in spatial data mining, CRC Press, Boca Raton

Stein A, Budde P, Yifru MZ (2009) A stereological estimator for the area of flooded land, International Symposium for Spatial Data Quality

Van de Vlag D, Stein A (2006) Uncertainty Propagation in Hierarchical Classification using Fuzzy Decision Trees. IEEE Transactions on Geoscience and Remote Sensing 45(1): 237–245

Vedel Jensen EB (1998) Local Stereology. World Scientific Publishing, Singapore

Yifru MZ (2006) Stereology for Data Mining. Unpublished MSc thesis, ITC International Institute for Geoinformation Science and Earth Observation, Enschede, The Netherlands